

Article

Internal Flow Characteristics of Centrifugal Pumps under Different Startup Combination Schemes

Xiaobo Zheng¹, Wei Wang¹, Pengli Zhang², Yongjian Pu¹ and Yaping Zhao^{1,*}

¹ Institute of Water Resources and Hydropower, Xi'an University of Technology, Xi'an 710048, China; zxb@xaut.edu.cn (X.Z.); 2220420038@stu.xaut.edu.cn (W.W.); 2200420102@stu.xaut.edu.cn (Y.P.)

² Hanjiang to Weihe River Valley Water Diversion Project Construction Co., Ltd., Xi'an 710024, China; xazpl@163.com

* Correspondence: zyp0168@xaut.edu.cn

Abstract: Pump station engineering is a water conservancy project used for long-distance water transfer, irrigation and drainage, and urban living and industrial water supply. Centrifugal pumps are one of the main pump types commonly used in pumping stations, and their operation is of considerable importance for the safety, stability, and efficient operation of pumping stations. This paper takes a large pumping station with seven centrifugal pump units as the research object and combines experimental research and numerical simulation. The axial flow velocity uniformity, average cross-sectional deviation angle, and hydraulic loss of the pump inlet section are evaluated, and the internal flow characteristics of the pump under different startup combination conditions are analyzed based on entropy generation and vorticity. This study also explores the operational performance of the pump station under different startup combination conditions, revealing the mutual influence mechanism between different startup combinations of pump stations and the internal and external characteristics of centrifugal pumps and introducing the optimal startup combination scheme for the pump station system. Research results indicate that the difference in energy loss of centrifugal pumps under different startup combinations is mainly manifested in the impeller and guide vane flow channels. For the two existing inlet flow channel structures in the pump station, the unit effectively operates when the inlet flow channel is tilted to the left. The optimal startup combination method of the pump station under different startup combinations is determined.



Citation: Zheng, X.; Wang, W.; Zhang, P.; Pu, Y.; Zhao, Y. Internal Flow Characteristics of Centrifugal Pumps under Different Startup Combination Schemes. *Water* **2024**, *16*, 1087. <https://doi.org/10.3390/w16081087>

Academic Editor: Helena M. Ramos

Received: 27 February 2024

Revised: 30 March 2024

Accepted: 4 April 2024

Published: 10 April 2024



Copyright: © 2024 by the authors. Licensee MDPI, Basel, Switzerland. This article is an open access article distributed under the terms and conditions of the Creative Commons Attribution (CC BY) license (<https://creativecommons.org/licenses/by/4.0/>).

Keywords: pump station; centrifugal pump; internal flow characteristics; startup combinations

1. Introduction

Considering the total water resources of China, despite the uneven spatial and temporal distribution, the “14th Five-Year Plan” proposes the following to solve the increasingly tense water resource phenomenon: “to be based on the basin as a whole and the spatial balance of water resources allocation”. Pumping station projects aim to provide an effective means for achieving the aforementioned goal. Therefore, the safe, stable, and efficient operation of pumping stations is also a concern. Most of the large pumping stations are generally installed with the same hydraulic characteristics as the pump unit. Thus, in the same flow and head conditions, the pumping station of the optimal combination of power on and the optimal operating conditions can help realize the minimum total energy consumption of the pumping station or its maximum total efficiency [1–3].

For the pumping station system, different start combinations and sequences have a remarkable impact on the pump inflow, which, in turn, will induce changes in the internal flow state of the pump. At present, numerous experts and scholars have conducted relevant research on the start combination of multi-unit pumping stations. Mahdi et al. [4] optimized the operating cost and efficiency of the pumping station based on the combination of high-efficiency pumps and the selection of pump types and established an optimization model.

Chang Pengcheng et al. [5] simulated the lateral inlet forebay of a multi-unit pumping station and found that its original model had a wide range of vortices inside the inlet pool. Xu Cundong et al. [6] studied the changing law of the flow pattern of the forebay under different combinations of switching on. They found that the best flow pattern improvement of the forebay in the lateral pumping station unit lies in the symmetrical switching on of the unit. Wu Peifeng et al. [7] used numerical simulation to analyze the symmetrical distribution of unit intake flow pattern in Dazhai River lock station. Their results revealed that two centered pumping station units arranged on each side of the unit intake conditions are highly favorable. Manuel et al. [8] proposed an optimal pump scheduling algorithm based on the ant colony algorithm, with the number of pumping station startups and the startup time as the optimization variables. Zidan et al. [9] studied different startup combinations and the distribution of sediment concentrations in the intake system. They found that when the number of start units increases, the sediment concentration on the sidewalls on both sides of the intake system decreases; when the units close to the wall do not operate, the sidewall area will appear as a dead water or vortex zones, which increases the sediment concentration. Wang Weilin [10] studied the hydraulic characteristics of the two lake sections of the terrace pumping station through hydraulic simulation to address the optimal efficiency of the switching machine and unit flow combination of the pumping station. He Yong et al. [11] numerically simulated the flow field in the front pool of the pumping station under different startup combinations and proposed the optimal startup combination scheme by combining the distribution uniformity of the water flow and the undesirable flow conditions such as vortex and walling off. Li Yingchun [12] conducted numerical simulations of the flow pattern in the forebay under different start combinations and combined the flow uniformity with the distribution of undesirable flow patterns to obtain the optimal startup combination scheme under high flow conditions. Qi Dunzhe et al. [9] studied the operating performance of the pumping station under different numbers of start units and found that increasing the number of start units worsens the operating performance of the pumping station. Guohui Cong et al. [13] investigated the vortex structure in the intake pool of the pumping station for different water levels and pump combinations and discovered the location and intensity of the vortex in different conditions. Wang et al. [14] developed a mathematical model to solve the problem of large energy consumption of the start–stop scheme in the pumping station. Chen et al. [15] combined numerical simulation and experimental research to analyze the hydraulic characteristics of the pumping station intake pool with an eccentric outlet. They found poor flow patterns in the intake pool and optimized these patterns by adding a flow-guiding pier. M T Rahman et al. [16] combined numerical simulation and experiments to analyze the internal flow characteristics of centrifugal pumps and combined the simulation results with the experiments results to obtain the location and intensity of vortices under different operating conditions. Byskov et al. [17] studied the internal flow field of centrifugal pumps through the large vortex simulation and found that the impeller flowed best at the design condition. The flow distribution of fluid in each flow channel was mainly uniform, while that when the pump was under small flow conditions was homogeneous. The flow distributions in the impeller and fluid were both highly homogeneous when the pump was under small flow conditions. Numerous stall vortices appear in the impeller channel when the centrifugal pump is in the small flow condition, blocking the impeller channel. The simulation results are finally compared with the particle image velocimetry (PIV) test results, yielding a high similarity. Ding et al. [18] simulated the internal flow characteristics of the centrifugal pump by changing the outlet angle of the vanes and conducted an experimental validation. Their results showed that the hydraulic loss of the centrifugal pump increases with the outlet angle of the vanes with the rise of the flow rate.

The results of the above studies reveal that different startup combination conditions have an important impact on the operational performance of the pumping station. Therefore, for a specific pumping station system, the safe and stable operation of the pumping station is of considerable importance for analyzing the hydraulic performance of the pump-

ing station under the conditions of different startup combinations and studying the optimal startup combination scheme. A large pumping station is taken in this paper as the research object, and the hydraulic performance of the pump unit under different startup combinations is studied by combining experimental and numerical research methods. The internal flow and energy characteristics of the centrifugal pump under different startup combinations are analyzed to determine the optimal startup combination scheme of the pumping station system. This scheme provides theoretical guidance for the safe and efficient operation of the pumping station.

2. Research Background and Experimental Model

2.1. Research Background

This paper takes a large pumping station system in Yangxian County, Shaanxi, as the research object. The pumping station has a total storage capacity of 221 million m³ and a regulating storage capacity of 0.98 billion m³. The powerhouse of the pumping station is at the dam toe, which has a total of seven vertical single-stage, single-suction centrifugal pumps with a water-lift design of 108.5 m and a single-pump flow rate of 12.6 m³/s. Among these pumps, six are operational and one is on standby.

2.2. Model Pumping Station Test Stand

Considering the feasibility of conducting the test, owing to the large size of the pumping station system prototype, this paper is based on the similarity principle: that is, the Euler number E and the Strouhal number Sr are equal, and the ratio of the size of the prototype pump to that of the model pump is 1:20. Sr and E are, respectively, defined as follows [19]:

$$Sr = \frac{D_2^3 n}{Q}, \quad (1)$$

$$E = \frac{gH}{D_2^2 n^2}, \quad (2)$$

where D_2 indicates the impeller outlet diameter (m); n denotes the rotational speed, (r/min); Q is the flow (m³/s); g is the acceleration of gravity (m/s²); and H is the head of the pump (m).

According to similarity theory, the parameter conversion relationship between the prototype and model pumps is shown in the following equation:

$$\frac{Q_p}{Q_m} = \frac{D_{2p}^3 n_p}{D_{2m}^3 n_m}, \quad (3)$$

$$\frac{H_p}{H_m} = \frac{D_{2p}^2 n_p^2}{D_{2m}^2 n_m^2}, \quad (4)$$

where the subscripts p and m represent prototype and model pumps, respectively.

The model test device comprises the forebay, circulating water supply pipe, model pump, electromagnetic flowmeter, flow control valve, water pump, and outlet pond. The model is generally transparent plexiglass, and its specific parameters are as follows: impeller inlet diameter of 74.67 mm, impeller outlet diameter of 138.67 mm, and rated speed of 1500 r/min. Figures 1 and 2 show the model test device and the site layout.

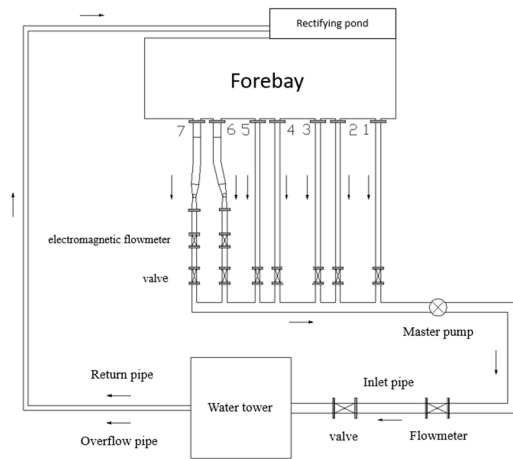


Figure 1. Schematic diagram of the overall model device. (1–7 is the pipe number).

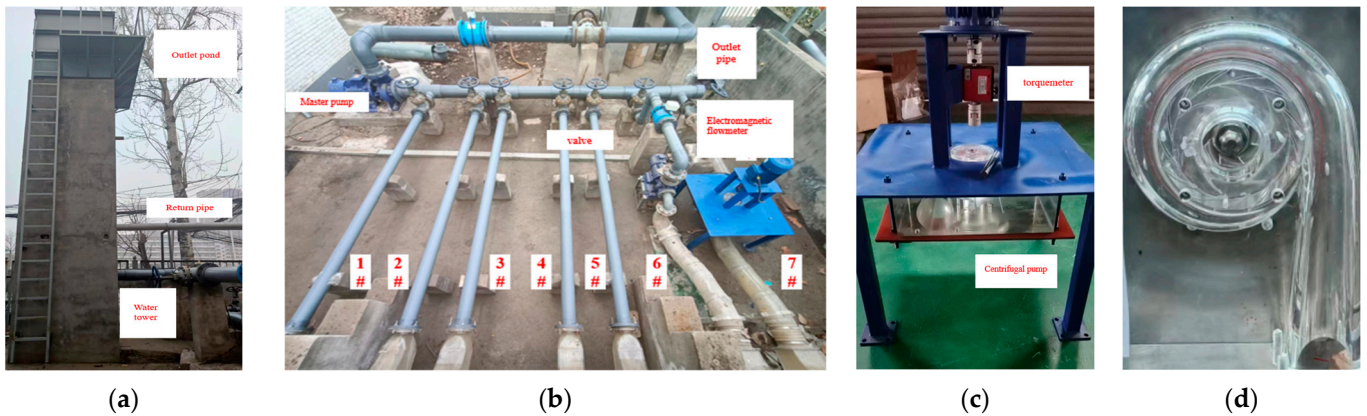


Figure 2. Model site layout. (a) The layout of water towers, return pipes, and outlet pond. (b) The layout of pumps, outlet pipes, and electromagnetic flowmeter. (c) Torquemeter and centrifugal pump. (d) Centrifugal pump. (1#–7# is the pipe number).

3. Numerical Calculation Method

3.1. Computational Modelling and Meshing

Figure 3 shows the numerical calculation area in this study, which contains the pumping station intake sump, inflow runner, seven vertical single-stage single-suction centrifugal pumps (impellers, guide vanes, and spiral casing), and the discharge pipe.

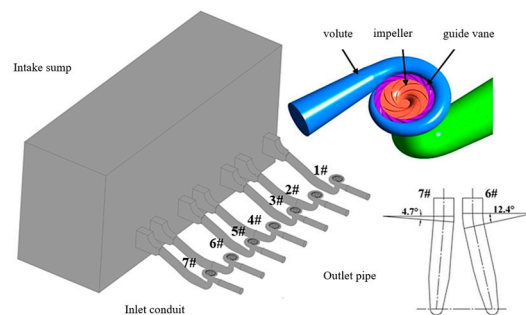


Figure 3. Geometric model of the model pumping station. (1#–7# is the pipe number).

The pumping station prototype single-pump design flow rate is $12.6 \text{ m}^3/\text{s}$, the design of the water lift is 108.5 m, the maximum water lift is 116.5 m, and the minimum water lift is 100.9 m. According to similar theoretical conversions of a single-pump design with a flow rate of $22.68 \text{ m}^3/\text{h}$, the design of the water lift is 4.34 m, the impeller inlet and outlet

diameters are 74.67 and 138.67 mm, respectively, and the rated speed is 1500 r/min. The shaped inlet passage of the elbow draft tube has two forms: one is 4.7° to the left of the central axis (units 1, 3, 5, and 7), and the other is 12.4° to the right of the central axis (units 2, 4, and 6).

The hexahedral mesh is used in this study to mesh each flow pump component to select the appropriate number of meshes that can guarantee the calculation accuracy and avoid the slow calculation speed. Under the design condition, with the pump head as the judgment index, the centrifugal pump unit section (including the intake sump, inflow runner, impeller, guide vane, spiral casing, and outlet pipe section) for a single unit of the mesh-independent verification calculations is shown in Figure 4. The figure reveals that the change in pump head amplitude is small and stable when the number of grids is 3.2 million in terms of the calculation cycle and the calculation capability. Finally, the number of grids is 4.26 million to complete the calculation after the grid distribution of various parts of the overcurrent, as shown in Figure 5.

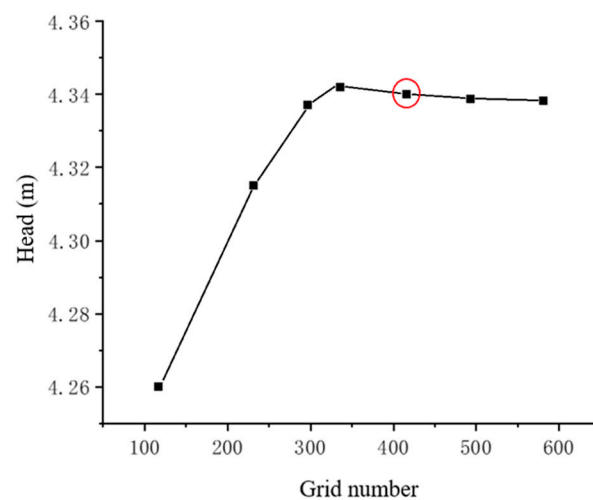


Figure 4. Grid-independent validation. (The red circle is the final number of meshes).

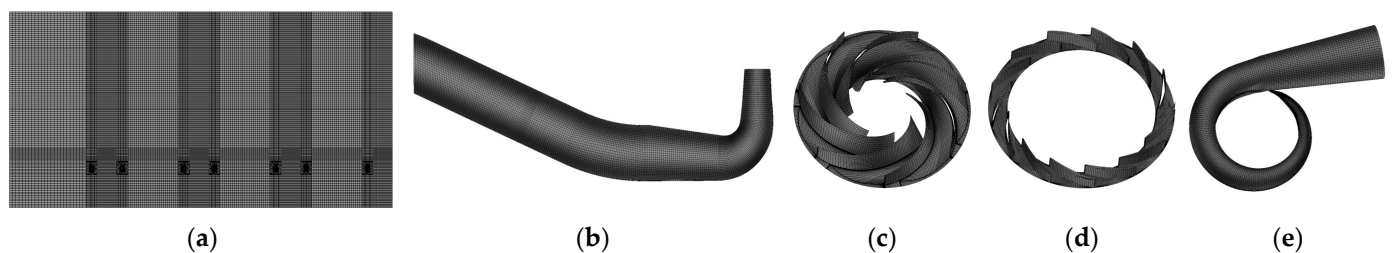


Figure 5. Grid schematic diagrams of each flow pump component. (a) Forebay grid; (b) inflow runner grid; (c) impeller grid; (d) guide vane grid; and (e) volute grid.

3.2. Numerical Calculation Model

With the pumping station centrifugal pump to water as the working medium, incompressible flow in the heat exchange calculation can be ignored, and only the continuity and momentum equations are considered [20].

(1) Continuity equation:

$$\frac{\partial \rho_m}{\partial t} + \frac{\partial (\rho_m u_i)}{\partial x_i} = 0, \quad (5)$$

where ρ is the fluid density (kg/m^3), t is the time (s), and u_i is the velocity tensor (m/s).

The research fluid in this paper is an incompressible fluid. Thus, the fluid density will not change with time, and the density remains constant. Equation (5) can then be simplified as follows:

$$\text{div}(\rho u) = 0, \quad (6)$$

(2) Momentum equation:

$$\frac{\partial(\rho u_i)}{\partial t} + \frac{\partial(\rho u_i u_j)}{\partial x_j} = -\frac{\partial p}{\partial x_i} + \frac{\partial}{\partial x_j} \left(\mu \frac{\partial u_i}{\partial x_j} - \rho \overline{u'_i u'_j} \right) + S_i, \quad (7)$$

where p is the pressure on the microbody (Pa), μ is dynamic viscosity (Pa·s), $-\rho \overline{u'_i u'_j}$ is the Reynolds stress (N), and S_i is the generalized source term.

A Reynolds stress term in the Reynolds-averaged Navier–Stokes equation remains unknown in the calculation of numerical simulation; thus, the turbulence model must be introduced when inserting the equations [21]. The issue studied in this paper belongs to the actual large-scale engineering problems; therefore, the standard model can be used to meet the computational requirements [22].

Numerical simulation software ANSYS (<https://www.ansys.com/>) is used in this paper to solve the flow field, and the boundary conditions and physical parameters are set as follows: the selected fluid medium is 25 °C water, the mass flow inlet is set at the inlet of the forebay, the flow rate changes with the number of startup units, and the specified value is 6.28 kg/s under the design condition of a single unit. Based on several pumping station calculation examples, the boundary condition at the outlet of the pumping station is selected as the hydrostatic outlet and set to a standard atmospheric pressure. The rotational speed is 1500 r/min. The grid interface is connected by a general grid interface (GGI) grid, and the convergence accuracy is 10^{-4} with a maximum residual.

4. Internal Flow Characteristics of Centrifugal Pumps under Different Combinations of Start Conditions

A certain deflection angle in the water flow from the forebay into the pumping station intake sump will result in poor flow conditions, thereby inducing deterioration of the pump suction conditions. Therefore, in the study of startup combinations, the most economical and reasonable startup scheme is selected, the inlet water flow pattern is improved, and the stable operation of the pumping unit is then ensured. This paper selects the section flow uniformity and the average deflection angle as the evaluation indexes (good or poor) of water flow in the flow channel. The value of the axial flow uniformity of the section is close to 1, while the value of the average deflection angle is close to 0° , which indicates that the axial flow velocity distribution of the pump impeller inlet section is highly uniform: vertical water flow into the pump leads to superior inlet conditions of the internal flow of the water pump [23].

The flow velocity uniformity λ of the water pump section is

$$\lambda = \left[1 - \frac{1}{\bar{v}_a} \sqrt{\frac{\sum (v_{ai} - \bar{v}_a)^2}{m}} \right] \times 100\%, \quad (8)$$

where: λ —inlet section axial flow uniformity, %; \bar{v}_a —average axial velocity of inlet section, m/s; m —number of calculation units in the inlet section; v_{ai} —axial velocity of unit i of the inlet section, m/s.

The average deflection angle of pump section θ is computed as follows:

$$\theta = \frac{\sum v_{ai} \left[\arctan\left(\frac{v_{ti}}{v_{ai}}\right) \right]}{\sum v_{ai}}, \quad (9)$$

where: θ —mean cross-section deflection angle, °; v_{ti} —axial velocity of unit i of the inlet section, m/s; $v_{ti} = \sqrt{v_{wi}^2 + v_{ri}^2}$ (v_{wi} , v_{ri} are the tangential and radial velocities of the i unit of the inlet section, respectively).

When more than one pumping unit simultaneously runs in the pumping station, the inlet conditions between different units vary, affecting the flow pattern of adjacent or separated pumping units. This paper aims to identify the economic and stable start conditions of multi-unit pumping stations. Numerical simulation and experimental analysis of all different start combinations of opening two, three, four, five, and six units are conducted, and the inlet cross-section of the pumps is selected as the characteristic cross-section. The most economical combination of operating conditions is determined by combining the evaluation indexes of various schemes, the flow velocity distribution of the characteristic cross-section, as well as the entropy production and vortex volume distribution. The velocity cloud diagram, entropy production diagram, and vorticity diagram were obtained through ANSYS. The velocity cloud diagram represented the velocity distribution of the inlet section of the pump, and the entropy production diagram and vorticity diagram represented the flow pattern of the inlet section of the pump.

4.1. Parallel Operation of Two Units

All the start combination conditions are simulated during the operation of the two units, and experimental tests on the hydraulic losses in the inlet section of the pumping station are simultaneously conducted. Figure 6 shows the distribution of flow uniformity and average deflection angle of the cross-section for different start combination scenarios. Figure 7 shows the distribution of hydraulic losses in the inlet section of the pumping station for different start combination scenarios and the total hydraulic losses.

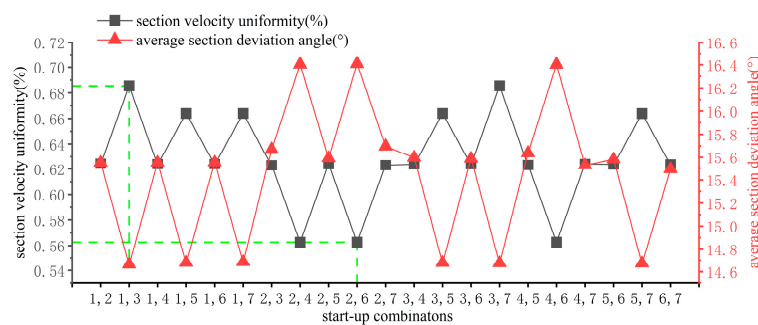


Figure 6. Uniformity of flow velocity and average section deviation angle distribution of cross-section for different start-up combination schemes. (The dotted line represents the coordinates of the point).

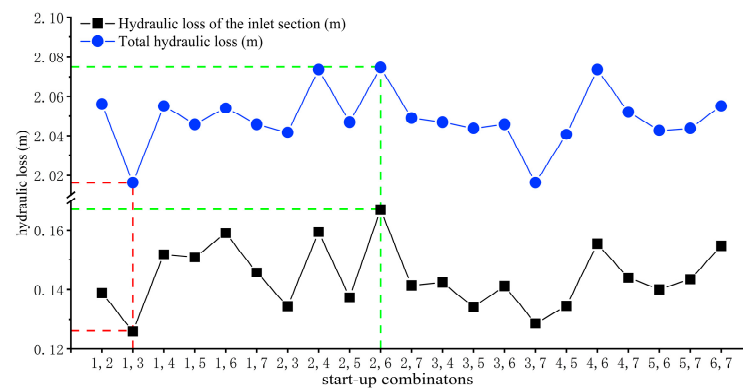


Figure 7. Hydraulic loss of the inlet section and total hydraulic loss of the pump station system for two units operating. (The dotted line represents the coordinates of the point).

The figures show that for two units running simultaneously, opening units 1 and 3 as well as 3 and 7 of the evaluation indexes are almost the same, demonstrating a flow rate uniformity of up to 68.55%. Opening units (2, 4), (2, 6), and (4, 6) of the evaluation index are no different. In these units, the flow rate uniformity is the lowest at 56.27%, the section flow rate uniformity of the maximum value and the minimum difference is within 12.28%, and the change in average cross-section deflection angle is minimal. The difference in maximum and minimum values is only 1.75° . The cross-section flow rate uniformity of the law of change and the pump unit hydraulic loss law are different from the law of change. When units 1 and 3 are switched on, the total hydraulic loss is the smallest (2.016 m); when units 2 and 6 are switched on, the total hydraulic loss is the largest (2.075 m). According to the test and simulation results, when the pumping station needs to switch on two units, the priority is to switch on the unit combination with the inlet flow path deviated to the left. Thus, the benefits of units 1 and 3 are optimal at this time. However, the benefits are worse when switching on the units with the right deviation of the inlet flow path. Meanwhile, the benefits of units 1 and 3 are optimal. The benefit is worse when the inlet flow path deviates to the right, and the worst benefit is achieved when the combination of units 2 and 6 is switched on.

Figure 8 shows the cross-section flow velocity distributions for the worst startup combination for units 2 and 6 and the best startup combination for units 1 and 3. Under the operating conditions of the two units, the following conditions are observed. When the inlet runner is switched on to the left of the unit, the corresponding flow velocity distribution area is average. When the inlet runner is switched on to the right of the unit, the flow velocity near the wall changes abruptly (high flow velocity is suddenly reduced to 0), and a large area of low-speed zone emerges at the wall, which is prone to cause water disturbance and induces an unstable flow, resulting in the emergence of vortex and increasing hydraulic losses. Differences in the flow state in the intake pipe will inevitably lead to variations in energy distribution within the pump.

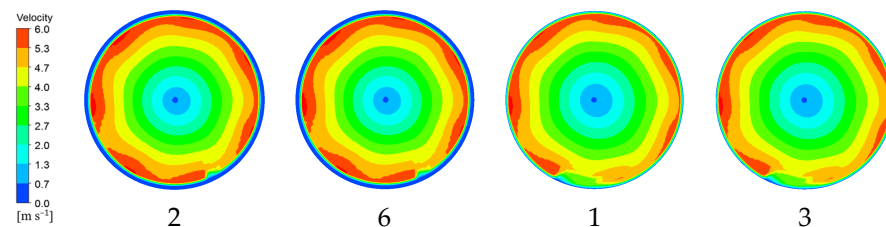


Figure 8. Velocity cloud diagram of characteristic section.

Figures 9 and 10, respectively, show the entropy production and vortex distribution in the middle section of the main overflow parts (impeller, guide vane, spiral casing) of the centrifugal pump with the optimal and worst combinations when two units are simultaneously switched on. The analysis shows that under the same working conditions, different combinations of opening the centrifugal pump affect its operating performance. In the impeller channel, the impeller energy loss is mainly concentrated in the impeller outlet due to the dynamic and static interferences between the impeller and guide vane, and local high entropy production area also occurs in individual impeller channels. In the guide vane and the spiral case, the energy loss is mainly concentrated in the guide vane flow channel due to the impingement of the high-speed flow of the fluid medium on the guide vane blades and the flow disorder due to the dynamic and static interferences between the guide vane and the impeller. The suction surface of the blade produces a local low-pressure area, thus forming a reverse pressure gradient; under the action of centrifugal force, the suction surface of the impeller flow separation phenomenon generates a vortex. Numerous vortices are generated at the inlet of the guide vane, which impedes the flow of water in the flow channel, resulting in increased energy loss. The entropy production value at this time is higher than that at the impeller, indicating that the energy loss at the guide vane is higher than the energy loss in the impeller. Compared with the worst start combination, the

entropy production value of the optimal start combination is remarkably reduced, and the vortex volume is also remarkably smaller than the worst start combination. This finding indicates that when the optimal start combination of units 1 and 3 is switched on, the fluid flow is relatively stable, and the flow loss is small. Overall, when two units must be switched on, priority is given to switching on units 1 and 3.

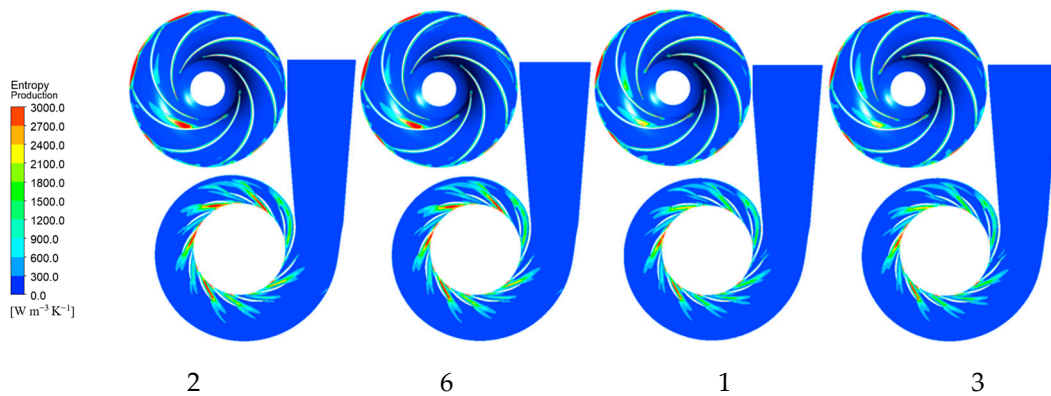


Figure 9. Distribution of entropy production of centrifugal pump’s main overflow parts when two units are turned on.

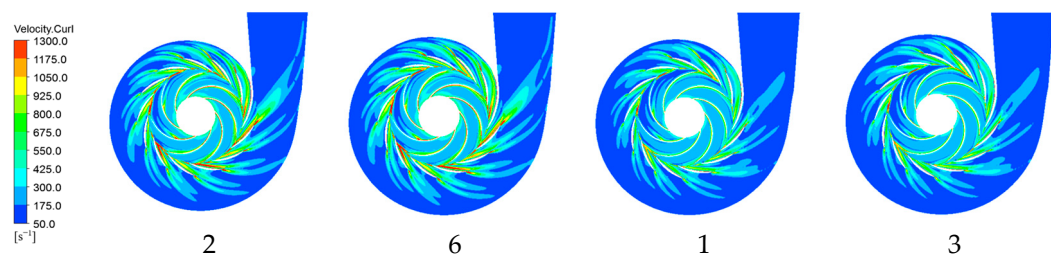


Figure 10. Vorticity cloud diagram of main flow components of centrifugal pump when two units are started.

4.2. Three Units in Parallel Operation

Figures 11 and 12 show the distribution of section flow uniformity and average section deviation angle as well as the distribution of hydraulic losses in the inlet section and total hydraulic losses for different start combination scenarios when the three units are operated in parallel.

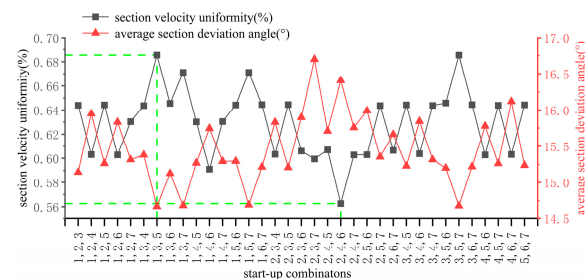


Figure 11. Uniformity of flow velocity and average section deviation angle distribution of cross-section for different start-up combination schemes. (The dotted line represents the coordinates of the point).

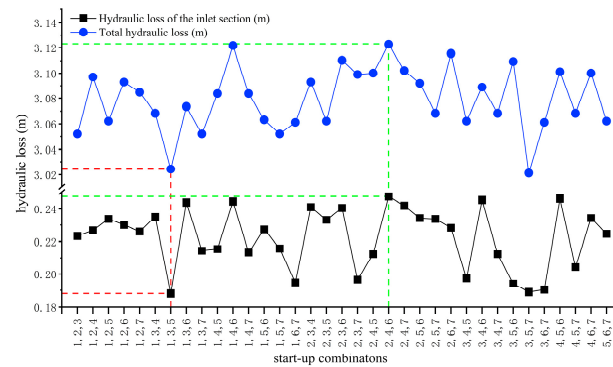


Figure 12. Hydraulic loss of the inlet section and total hydraulic loss of the pump station system for three units operating. (The dotted line represents the coordinates of the point).

According to the calculation results, for three units running simultaneously, opening units 1, 3, and 5 as well as 3, 5, and 7 of the evaluation indexes are almost the same, revealing the highest flow rate uniformity of up to 68.54%. Meanwhile, opening units 2, 4, and 6 yields the lowest flow rate uniformity of 56.27%. The maximum and maximum values of the section flow rate uniformity demonstrated a difference of 12.27%. The relative change in the average cross-section deflection angle is minimal. The difference in maximum and minimum values is only 2.03°. Cross-section flow rate uniformity of the law of change and the pumping unit hydraulic loss law is different from the law of change: opening units 3, 5, and 7 yielded the smallest total hydraulic loss of 3.021 m, while opening units 2, 4, and 6 produced the largest total hydraulic loss of 3.123 m. The test and simulation results of the trend are the same. When units 1, 3, and 5 are opened, the difference in maximum and minimum values is 12.27%. The hydraulic loss in the inlet section of the pumping station system is the smallest (0.1882 m) when units 1, 3, and 5 are switched on. In contrast, the hydraulic loss in the inlet section of the pumping station system is the largest (0.2473 m) when units 2, 4, and 6 are switched on.

Figure 13 shows the characteristic cross-sectional flow velocity distributions for the worst startup combination (opening units 2, 4, and 6) and the optimal startup combination (opening units 1, 3, and 5). The characteristic cross-section flow velocity plots reveal that, under the operating conditions of three units, the corresponding flow velocity distribution is better when the unit with the inlet runner to the left is switched on than when the unit with the inlet runner to the right is switched on. Compared with switching on two units simultaneously, the uniformity of flow velocity in the characteristic cross-section of switching on three units simultaneously is almost unchanged.

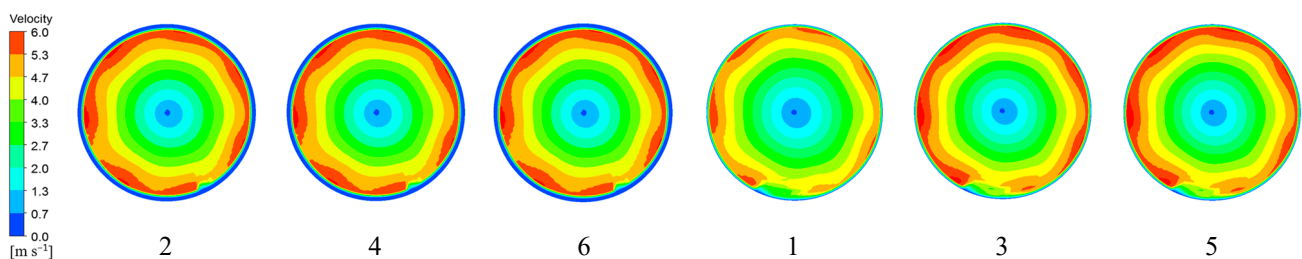


Figure 13. Velocity cloud diagram of characteristic section.

Figure 14 reveal the entropy production inside the centrifugal pump. Figure 15 shows the entropy production distribution of the main overflow parts (impeller, guide vane, volute) in the middle section of the centrifugal pump for the optimal and worst combinations when three units are switched on simultaneously. Compared with switching on two units simultaneously, the entropy production in the flow channel of the main overflow parts of the centrifugal pump is increased when the three units are switched on simultaneously.

Therefore, when the three units are simultaneously switched on, the energy loss inside the centrifugal pump is larger than when the two units are simultaneously switched on; the optimal start combination is smaller than that of the worst start combination compared with that of the optimal start combination. The optimal start combination has a smaller entropy production value than the worst start combination in the impeller channel and the channel near the nose of the spiral case. The maximum value of the vortex distribution of the centrifugal pump when three units are switched on is mainly concentrated in the impeller suction surface and guide vane inlet and flow channel. Meanwhile, the vortex of the worst combination significantly increases in the impeller channel near the wall of the vane suction surface, as well as in the guide vane flow channel and the spiral casing near the outlet of the guide vane. The vortex increase is particularly observed in the guide vane flow channel. The flow of the optimum combination is better than that of the worst combination in all flow channels. Therefore, when three units must be switched on, priority is given to switching on units 1, 3, and 5.

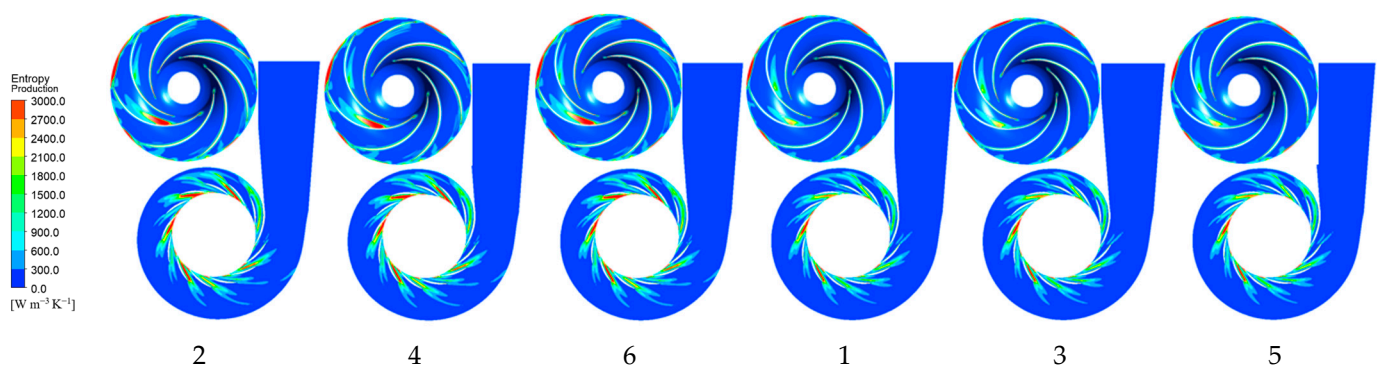


Figure 14. Entropy production distribution cloud diagram of main flow parts of the centrifugal pump when three units are operated.

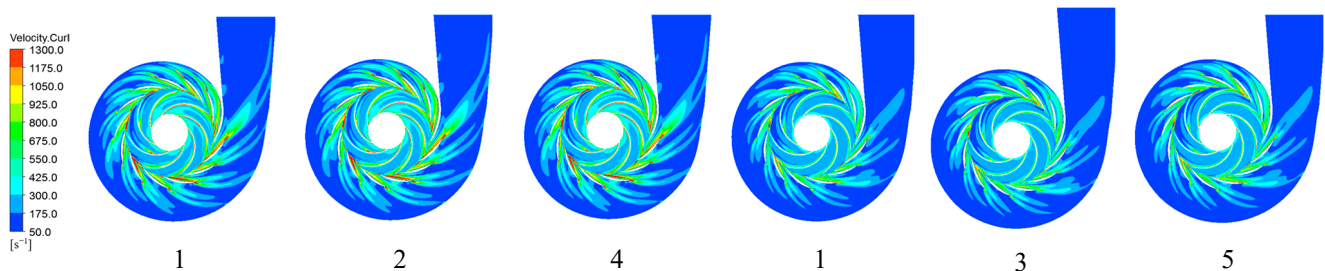


Figure 15. Vorticity cloud diagram of main flow components of the centrifugal pump when three units are started.

4.3. Parallel Operation of Four Units

All the start combination conditions are simulated in this paper during the operation of the four units. Figure 16 shows the calculation results of the four units. Meanwhile, Figure 17 reveals the distribution of hydraulic and total hydraulic losses in the inlet section of the pumping station during the operation of the four units.

According to the calculation results, for the case of four units running simultaneously, the flow rate uniformity is the highest when units 1, 3, 5, and 7 are opened, reaching 67.49%. The flow situation is similar when the following units are opened: 1, 2, 4, and 6; 2, 3, 4, and 6; 2, 4, 5, and 6; 2, 4, 6, and 7. When flow rate uniformity is the lowest at 59.32%, the difference in flow velocity section uniformity of the maximum and minimum values is 8.17%. Meanwhile, the average cross-section deflection angle of the relative change is minimal, and the difference in the maximum and minimum values is only 1.50°. The cross-section flow rate uniformity of the law of change and the pump unit hydraulic loss

law is different from the law of change. When units 1, 3, 5, and 7 are switched on, the total hydraulic loss is the smallest at 4.06628 m; when units 1, 2, 4, and 6 are switched on, the total hydraulic loss is the largest at 4.1318 m. The test and numerical simulation results demonstrate the same trend: when units 1, 3, 5, and 7 are switched on, the hydraulic loss of the pumping station system inlet section is the smallest at 0.2535 m; when units 1, 2, 4, and 6 are switched on, the hydraulic loss of the pumping station system inlet section is the largest at 0.3479 m.

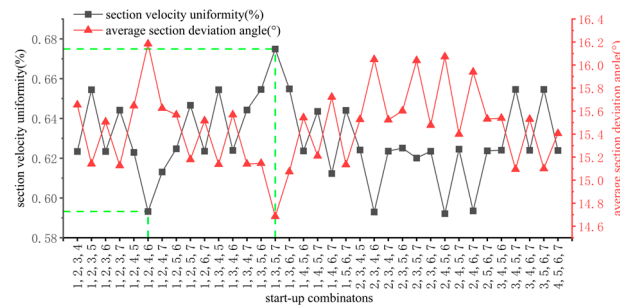


Figure 16. Uniformity of flow velocity and average section deviation angle distribution of cross-section for different start-up combination schemes. (The dotted line represents the coordinates of the point).

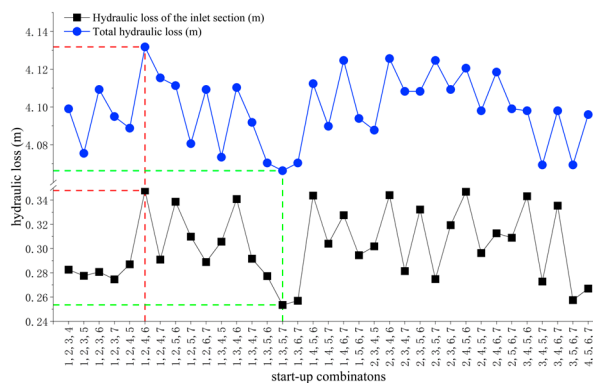


Figure 17. Hydraulic loss of the inlet section and total hydraulic loss of the pump station system for four units operating. (The dotted line represents the coordinates of the point).

Figure 18 shows the characteristic cross-section flow velocity distribution cloud plots for the worst startup combination, opening units 1, 2, 4, and 6, and the optimal startup combination, opening units 1, 3, 5, and 7. The characteristic cross-section flow velocity maps indicate the following: when the four units are operated, the corresponding flow velocity distribution area is better when the unit with the inlet runner to the left is switched on than when the unit with the inlet runner to the right is switched on. Compared with switching on three units simultaneously, no change in the flow uniformity in the characteristic section is observed when four units are simultaneously switched on. Figure 19 shows the entropy production distribution cloud diagram of the middle section of the main overflow parts (impeller, guide vane, volute) of the centrifugal pump with the optimal and worst combinations when four units are simultaneously switched on.

The entropy production of the centrifugal pump decreases when four units are simultaneously switched on compared with that when two and three units are switched on. This finding indicates that the mutual influence between the units gradually decreases at this time, the inlet conditions improve, and the energy loss is reduced. The optimal and worst combinations when four units are simultaneously switched on include unit 1. However, in the optimal combination, the entropy production of unit 1 is slightly smaller than that of the worst combination. This finding indicates that the inlet conditions of the centrifugal pumps are affected differently when varying units are switched on. Comparing units 2,

4, and 6 with units 3, 5, and 7, the high entropy production area of units 3, 5, and 7 in the optimal combination is significantly smaller than that of units 2, 4, and 6 in the worst combination. This result indicates that the internal flow of the centrifugal pumps under the conditions of the optimal combination is uniform and the energy loss is small. Compared with the worst startup combination, the entropy production value of the optimal startup combination is generally significantly reduced, and the vortex volume is also significantly smaller than the worst startup combination. This finding indicates that when opening the optimal combination of units 1, 3, 5, and 7, the fluid flow remains relatively stable, and the flow loss is small.

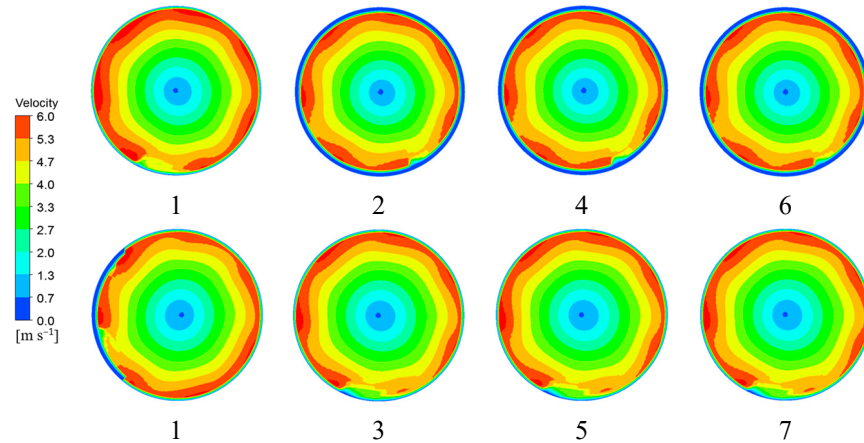


Figure 18. Velocity cloud diagram of characteristic section.

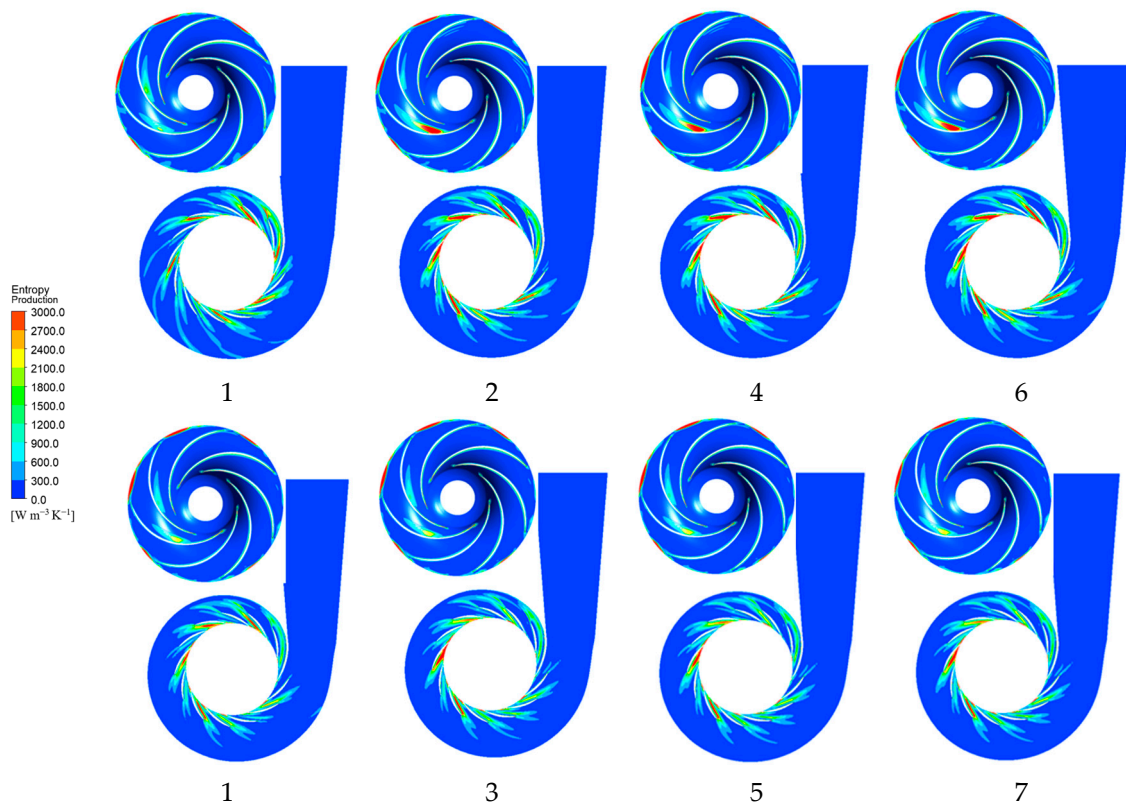


Figure 19. Entropy production distribution cloud diagram of the main flow parts of the centrifugal pump when four units are started.

Compared with the case when two and three units were simultaneously switched on, the vortices in the overflow components were reduced when four units were simultaneously

switched on. This phenomenon is consistent with the distribution of the entropy production values, indicating that the flow inside the centrifugal pump was more uniform when four units were simultaneously switched on than when two and three units were simultaneously switched on. Figure 20 shows that the worst combination for high vorticity area is more evident than the optimal combination. Overall, when four units must be switched on, priority is given to switching on units 1, 3, 5, and 7.

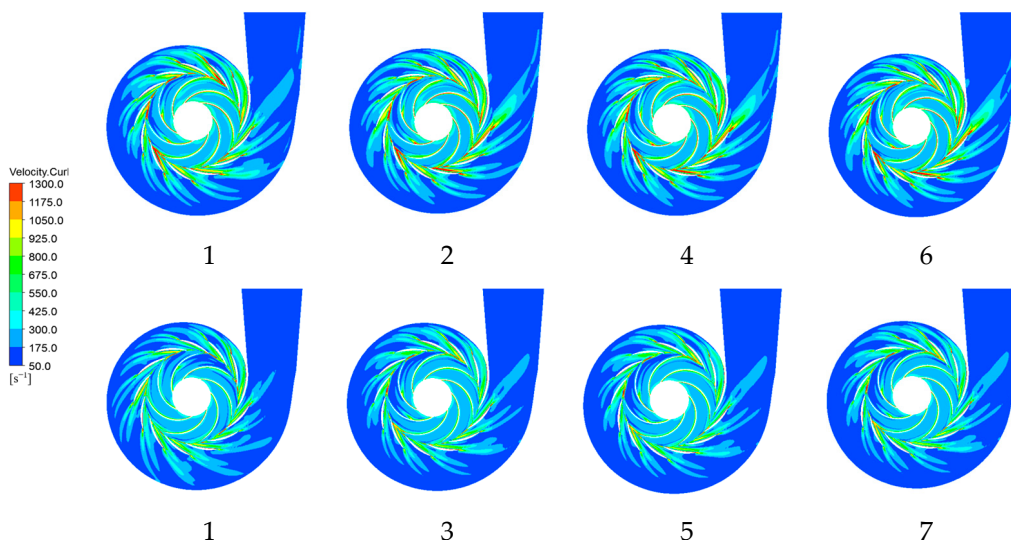


Figure 20. Vorticity cloud diagram of main flow components of the centrifugal pump when four units are started.

4.4. Parallel Operation of Five Units

The five units were simulated in this paper for all the start combinations of operating conditions. Figure 21 shows the specific start combination scheme and the calculation results. Meanwhile, Figure 22 shows the distribution of hydraulic and total hydraulic losses in the inlet section of the pumping station during the operation of five pumps.

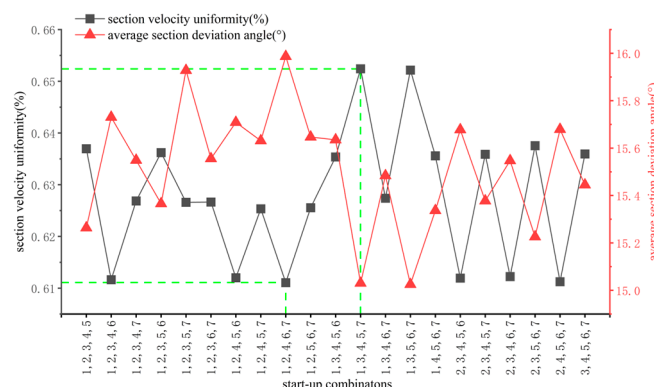


Figure 21. Uniformity of flow velocity and average section deviation angle distribution of cross-section for different start-up combination schemes. (The dotted line represents the coordinates of the point).

The calculation results reveal that for five units operating simultaneously, units 1, 3, 4, 5, and 7 are opened when the flow rate uniformity is the highest (up to 65.24%), while units 1, 2, 4, 6, and 7 are opened when the flow rate uniformity is the lowest (61.11%). The difference in maximum and minimum values of section flow rate uniformity is 3.93%, and the relative change in the average cross-section deflection angle is minimal. The difference between the maximum and minimum values is only 0.96°. Moreover, the change law of section flow rate uniformity and pump unit hydraulic loss change law is different from that

of the minimum total hydraulic loss. The difference between the maximum and minimum values is only 0.96° . The rule of change of section flow uniformity and pump unit hydraulic loss change law is also different: opening units 1, 3, 4, 5, and 7 yields the smallest total hydraulic loss of 5.10 m, while opening units 1, 2, 4, 6, and 7 leads to the largest total hydraulic loss of 5.15 m. Thus, the test and numerical simulation results demonstrate the same trend. Meanwhile, units 1, 3, 4, 5, and 7 are simultaneously opened when the pumps are not in the same position. The test has the same trend as the numerical simulation results. The hydraulic loss in the inlet section of the pumping station system is the smallest when units 1, 3, 4, 5, and 7 are switched on, and the hydraulic loss in the inlet section of the pumping station system is the largest when units 1, 2, 4, 6, and 7 are switched on. The hydraulic loss in the inlet section of the pumping station system is the largest (0.451 m) when units 1, 2, 4, 6, and 7 are switched on.

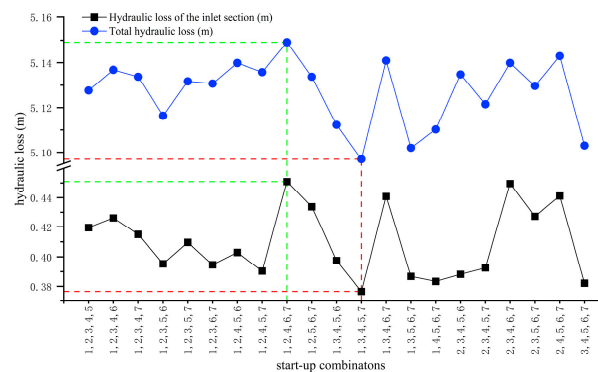


Figure 22. Hydraulic loss of the inlet section and total hydraulic loss of the pump station system for five units operating. (The dotted line represents the coordinates of the point).

Figure 23 shows the characteristic cross-section flow velocity distribution cloud diagrams for the worst startup combination (opening units 1, 2, 4, 6, and 7) and the optimal startup combination opening units (1, 3, 4, 5, and 7). It can be seen from the characteristic cross-section flow velocity maps that, under the operating conditions of five units, the corresponding flow velocity distribution area is better when the unit with the inlet runner to the left is switched on than when the unit with the inlet runner to the right is switched on. Compared with simultaneously switching on four units, the flow velocity distribution in the characteristic section of the worst combination is more uniform than that when five units are simultaneously switched on. The flow velocity uniformity in the section of the optimal combination is worse than that of switching on four units simultaneously. Therefore, when five units must be switched on, priority is given to switching on units 1, 3, 4, 5, and 7.

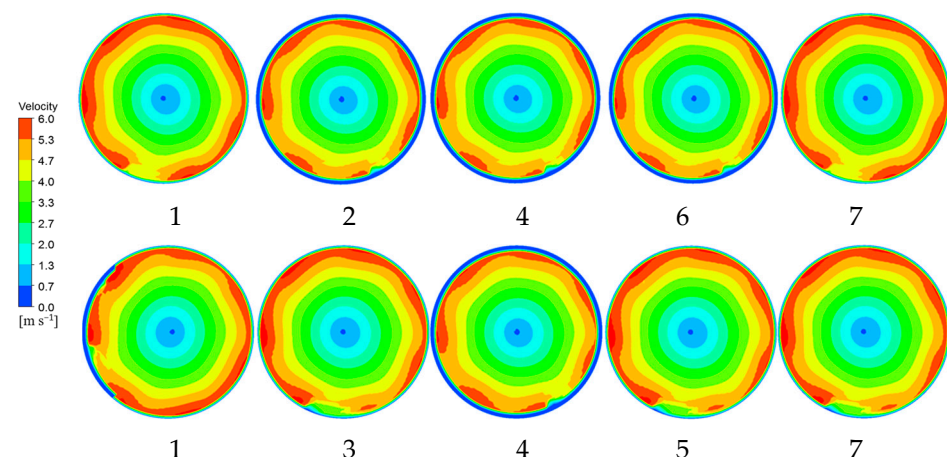


Figure 23. Velocity cloud diagram of characteristic sections.

4.5. Six Units in Parallel Operation

All the start combination conditions are simulated in this paper during the operation of six units. Figure 24 shows the specific start combination scheme and the calculation results. Meanwhile, Figure 25 shows the distribution of hydraulic losses in the inlet section of the pumping station and the total hydraulic losses during the operation of the six units.

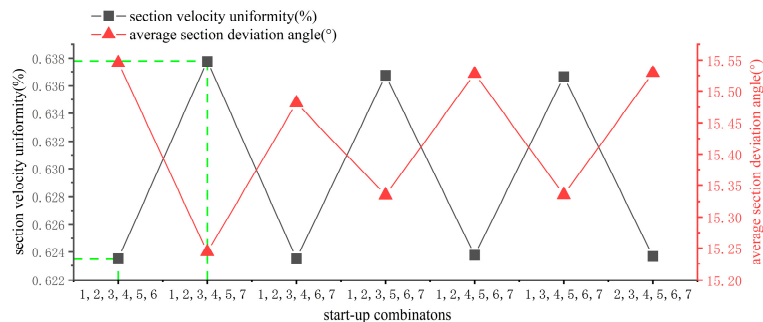


Figure 24. Uniformity of flow velocity and average section deviation angle distribution of cross-section for different start-up combination schemes. (The dotted line represents the coordinates of the point).

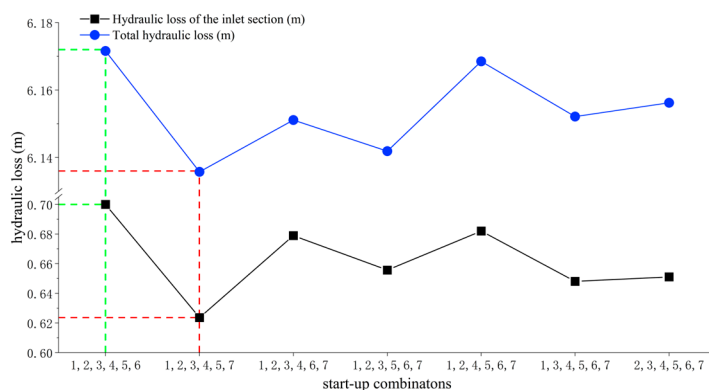


Figure 25. Hydraulic loss of the inlet section and total hydraulic loss of the pump station system for six units operating. (The dotted line represents the coordinates of the point).

The calculation results reveal that for the six units operating simultaneously, opening units 1, 2, 3, 4, 5, and 7 yields the highest flow rate uniformity of up to 63.78%, while opening units 1, 2, 3, 4, 5, and 6 results in the lowest flow rate uniformity of 62.35%. The difference between the maximum and minimum values of the section flow rate uniformity is 1.34%, and the relative change in the average cross-section deflection angle is minimal. The difference in the maximum and minimum values is only 0.3°. The change rule of the section flow rate uniformity and the pump unit hydraulic loss is different. When units 1, 2, 3, 4, 5, and 7 are switched on, the difference between the maximum and minimum values of total hydraulic loss is only 0.3°. The change rule of section flow uniformity is different from that of hydraulic loss of the pumping unit: when switching on units 1, 2, 3, 4, 5, and 7, the total hydraulic loss is the smallest (6.136 m); when switching on units 1, 2, 3, 4, 5, and 6, the total hydraulic loss is the largest (6.172 m). The test results reveal the same trend as the results of numerical simulations. When six units are simultaneously switched on, the hydraulic loss in the inlet section of the pumping station system is the smallest (0.6236 m) when units 1, 2, 3, 4, 5, and 7 are switched on, while the hydraulic loss in the inlet section of the pumping station system is the largest (0.7 m) when units 1, 2, 3, 4, 5, and 6 are switched on.

Figure 26 shows the characteristic cross-section flow velocity distribution cloud diagrams for the worst start combinations for switching on units 1, 2, 3, 4, 5, and 6 and the optimal start combinations for switching on units 1, 2, 3, 4, 5, and 7. The characteristic

cross-section flow velocity map reveals that when the six units are running, compared with the previous conditions, the flow velocity uniformity of the pump inlet cross-section and the average cross-section deflection angle do not demonstrate substantial changes. The cross-section cloud map is also maintained. Overall, when switching on the six units, priority is given to switching on units 1, 2, 3, 4, 5, and 7.

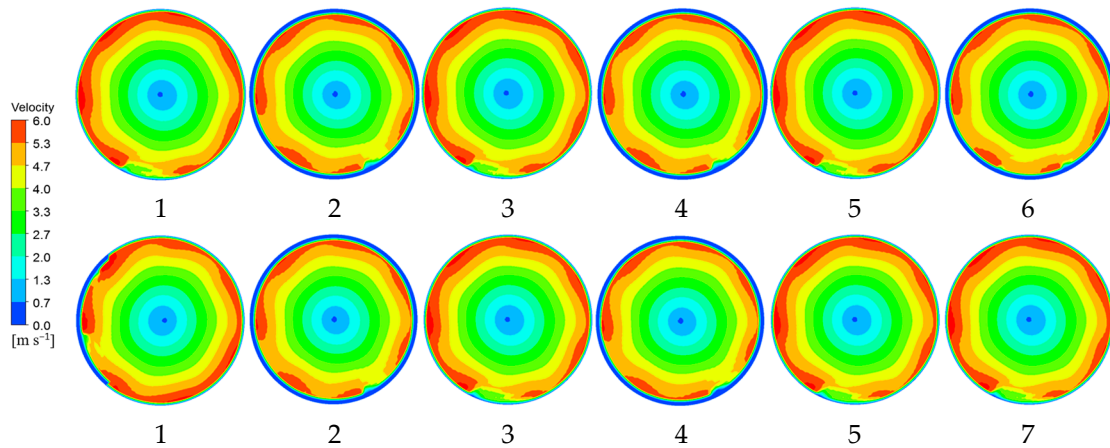


Figure 26. Velocity cloud diagram of a feature section.

5. Conclusions

In this paper, through the design of different scheme combinations under the number of starts, the simultaneous individual opening of two, three, four, five, and six units as well as other operating conditions is analyzed to calculate the axial flow velocity uniformity of the inlet section of the pump, the average section deviation angle, and the hydraulic loss. The pump is examined under different start combination conditions and pump flow characteristics to explore the opening of different numbers of units under the circumstances of economical start combinations. The following conclusions are obtained:

(1) When different numbers of units are running, the number of odd-numbered units compared to that of even-numbered units in the water conditions is superior, the section flow uniformity is high, and the average section deviation angle and hydraulic loss are small.

(2) The results of vortex and entropy maps of the impeller, guide vane, and the middle section of the volute show that the unstable flow in the centrifugal pump mainly occurs at the impeller outlet and in the guide vane runner. Therefore, the main energy loss of the centrifugal pump occurs in the vicinity of the impeller outlet and the guide vane runner. For different start combinations, the differences in the flow characteristics of the centrifugal pump are mainly reflected in the areas with the most severe undesirable flow, such as the impeller runner and the entire runner of the guide vane.

(3) Owing to the differences in the pumping station inlet conditions under different startup combinations, the overall combination of simulation calculations reveals the optimal startup scheme combination of pumping station systems as shown in Table 1: when two units are simultaneously switched on, priority is given to units 1 and 3; when three units are switched on, priority is given to units 1, 3, and 5; when four units are switched on, priority is given to units 1, 3, 5, and 7; when five units are switched on, priority is given to units 1, 2, 3, 5, and 7; when six units are simultaneously switched on, priority will be given to units 1, 2, 3, 4, 5, and 7.

Table 1. The optimal startup scheme combination of pumping station systems.

The Number of Units in Operation	The Optimal Startup Scheme
2	1, 3
3	1, 3, 5
4	1, 3, 5, 7
5	1, 2, 3, 5, 7
6	1, 2, 3, 4, 5, 7

Author Contributions: X.Z. and P.Z. conceived and supervised the study, and carried out the numerical simulations; Y.P. and W.W. conducted the experiment and wrote the first draft of the manuscript. X.Z. and Y.Z. carried out the data analysis and edited the manuscript. All authors have read and agreed to the published version of the manuscript.

Funding: This work was supported by the Joint Foundation of Shaanxi [Grant No. 2019JLP-25].

Data Availability Statement: Data are contained within the article.

Conflicts of Interest: P.Z. was employed by the Hanjiang-to-Weihe River Valley Water Diversion Project Construction Co., Ltd. The remaining authors declare that the research was conducted in the absence of any commercial or financial relationships that could be construed as a potential conflict of interest.

References

- Zhang, R.; Cheng, J.; Zhu, H.; Yao, L.; Zhang, L. Low-head Pump Performances and Determination of Reasonable Scope for Variable Speed Operation. *J. Ineragricult. Machy* **2009**, *40*, 78–81.
- Wu, H.; Zhou, Z.; Gao, Y.; Li, J. Research of Optimized Dispatching of Cascade Pumping Stations Based on Hydrodynamic Dispersion Model and Genetic Algorithm. *Haihe Water Resour.* **2014**, 46–49. Available online: https://www.alljournals.cn/view_abstract.aspx?pcid=5B3AB970F71A803DEACDC0559115BF0A068CD97DD29835&cid=3ECA06F115476E3F&jid=8D2FD083F0BFAB3C390FA3932AD11EAA&aid=34B6762159E1CD4D51FFED50B5A38286&yid=9EAD63ADE6B277ED (accessed on 1 April 2024).
- Lin, L. Optimised Scheduling of Pumping Station System Based on Genetic Algorithm. Master's Thesis, Tianjin University, Tianjin, China, 2007.
- Moradi-Jalal, M.; Mariño, M.A.; Afshar, A. Optimal Design and Operation of Irrigation Pumping Stations. *J. Irrig. Drain. Eng.* **2003**, *129*, 149–154. [[CrossRef](#)]
- Pengcheng, C.; Fan, Y.; Dandan, S.; Li, Z.B.; Shen, Q.R. Analysis of flow pattern and rectification measures in lateral inlet forebay of multi-unit pumping station. *China Rural Water Conserv. Hydropower* **2021**, *12*, 229–234.
- Xu, C.; Wang, R.; Liu, H.; Lian, H.; Wang, Y.; Wang, G. Research on the influence of start-up combinations on the flow pattern in forebay of side-in-let pumping station on sandy river. *J. Water Resour.* **2020**, *51*, 92–101.
- Wu, P.; Zhou, Q.; Ding, H.; Wang, Z.; Xu, J. Numerical simulation of inlet flow of symmetrically distributed units in Dazhai River. *Water Conservancy Sci. Technol. Econ.* **2021**, *27*, 68–70.
- Bagirov, A.M.; Barton, A.F.; Mala-Jetmarova, H.; Al Nuaimat, A.; Ahmed, S.T.; Sultanova, N.; Yearwood, J. Ant-Colony Optimization for Optimal Pump Scheduling. *Math. Comput. Model.* **2013**, *57*, 873–886. [[CrossRef](#)]
- Zi, D.; Wang, B.; Wang, F.; He, C.; Xue, S. Influences of start-up pump units on the sediment concentration for the intake system of a pumping station. *J. Agric. Eng.* **2022**, *38*, 59–68.
- Weilin, W. Research on the Optimal Operation of Terrace Pumping Station in Two Lakes Section. Master's Thesis, Jinan University, Jinan, China, 2020.
- He, Y.; Pan, Z.; Yu, H.; Qiu, S. Optimizatin on combination of pumping unit start-up for large pumping station under complicated flow pattern in fore bay. *Water Conserv. Hydropower Technol.* **2016**, *47*, 69–74.
- Li, Y.; Luo, W.; Li, C. An Analysis of Flow Pattern of Forebay and Units Commitment Optimization. *China Rural Water Hydropower* **2014**, 108–111. Available online: https://kns.cnki.net/kcms2/article/abstract?v=ttOPOQ75YvKtvHJwQyHY3aTJYH5e12cPUSvTuyOaLKJx6RvSfAONWbW2R2D7J0PPPh2UP5gZSN_Fqraky39xeLCEhQuuz9Ucb8T7xaQIIJfBbh5nUhCbUpp5vO7Ch43C&uniplatform=NZKPT&flag=copy (accessed on 1 April 2024).
- Guohui, C.; Fujun, W. Numerical investigation on the flow structure and vortex behavior at a large scale pump sump. In Proceedings of the Fluids Engineering Division Summer Meeting, San Diego, CA, USA, 30 July–2 August 2007.
- Wang, S.; Cheng, J.; Zhu, B. Optimal operation of a single unit in a pumping station based on a combination of orthogonal experiment and 0-1 integer programming algorithm. *Water Supply* **2022**, *22*, 7905–7915. [[CrossRef](#)]

15. Chen, Y.X.; Xi, B.; Chen, Z.; Shen, S. Study on the Hydraulic Characteristics of an Eccentric Tapering Outlet Pressure Box Culvert in a Pumping Station. *Processes* **2023**, *11*, 1598. [[CrossRef](#)]
16. Rahman, M.T.; Siddiqi, M.A. Study Involving the Flow Pattern Comparison of a PIV Experiment with CFD Simulation, for the Flow within a Centrifugal Pump. In Proceedings of the Fluids Engineering Division Summer Meeting, Chicago, IL, USA, 3–7 August 2014; American Society of Mechanical Engineers: New York, NY, USA, 2014; Volume 46216, p. V01AT07A006.
17. Byskov Rikke, K.; Jacobsen Christian, B.; Pedersen, N. Flow in a centrifugal pump impeller at design and off-design conditions—Part II: Large eddy simulations. *J. Fluids Eng.* **2003**, *125*, 73–83. [[CrossRef](#)]
18. Ding, H.; Li, Z.; Gong, X.; Li, M. The influence of blade outlet angle on the performance of centrifugal pump with high specific speed. *Vacuum* **2019**, *159*, 239–246. [[CrossRef](#)]
19. Zhang, K. *Principles of Fluid Machinery*; Mechanical Industry Press: South Norwalk, CN, USA, 2014.
20. Wang, F.; Tang, X.; Chen, X.; Xiao, R.; Yao, Z.; Yang, W. A review on flow analysis method for pumping stations. *J. Water Resour.* **2018**, *49*, 47–61.
21. Liu, W. Research on the Influence Law of Double Worm Shell Structure on the Radial Force of Centrifugal Pump Impeller. Master's Thesis, Lanzhou University of Technology, Lanzhou, China, 2018.
22. Zhou, S. Research on the Problem of solid-Liquid Two-Phase Flow Centrifugal Pump Erosion and Wear. Master's Thesis, Xi'an University of Technology, Xi'an, China, 2017.
23. Ming, L.; Yong, W.; Wei, X.; Erlin, W.; Houlin, L. Optimisation of geometric parameters of lateral inlet forebay of pumping station. *J. Agric. Eng.* **2022**, *38*, 69–77.

Disclaimer/Publisher's Note: The statements, opinions and data contained in all publications are solely those of the individual author(s) and contributor(s) and not of MDPI and/or the editor(s). MDPI and/or the editor(s) disclaim responsibility for any injury to people or property resulting from any ideas, methods, instructions or products referred to in the content.